

Enhancing Door-Status Detection for Autonomous Mobile Robots during Environment-Specific Operational Use

Michele Antonazzi, Matteo Luperto, Nicola Basilico, N. Alberto Borghese

Abstract—Door-status detection, namely recognizing the presence of a door and its status (open or closed), can induce a remarkable impact on a mobile robot’s navigation performance, especially for dynamic settings where doors can enable or disable passages, changing the topology of the map. In this work, we address the problem of building a door-status detector module for a mobile robot operating in the same environment for a long time, thus observing the same set of doors from different points of view. First, we show how to improve the mainstream approach based on object detection by considering the constrained perception setup typical of a mobile robot. Hence, we devise a method to build a dataset of images taken from a robot’s perspective and we exploit it to obtain a door-status detector based on deep learning. We then leverage the typical working conditions of a robot to *qualify* the model for boosting its performance in the working environment via fine-tuning with additional data. Our experimental analysis shows the effectiveness of this method with results obtained both in simulation and in the real-world, that also highlight a trade-off between costs and benefits of the fine-tuning approach.

I. INTRODUCTION

Autonomous mobile robots are nowadays increasingly employed for cooperating with humans in a variety of tasks settled in indoor public, private, and industrial workspaces. A challenge posed to these *collaborative robots* is coping with highly dynamic environments characterized by features that can rapidly and frequently change, very often due to the presence of human beings [1]. Consider, as examples, a domestic setup in an apartment or a workspace with several offices. In a time span of hours or days, the topology itself of these environments might frequently change its connectivity, since doors may be left open or closed, hence modifying in time the reachability of free spaces. This phenomenon strongly impacts the capability of robots to efficiently navigate and perform their tasks. At the same time, during their operational time, robots are often exposed to large amounts of data about their surroundings that offer an opportunity to track, model, and predict doors’ statuses (and topology variations). The relevance of this problem is well-established in the literature. Different works, such as [2], [3], show how modelling the status of doors across a long time span and predicting the changes in the environment topology improves a robot’s task performance. Intuitively, better paths can be planned by taking into account whether a room will be reachable or not upon arriving there.

Central to unlocking such enhanced indoor navigation behaviors is what we call in this work *door-status detection*: the robot’s capability to extract the location of a door *and*

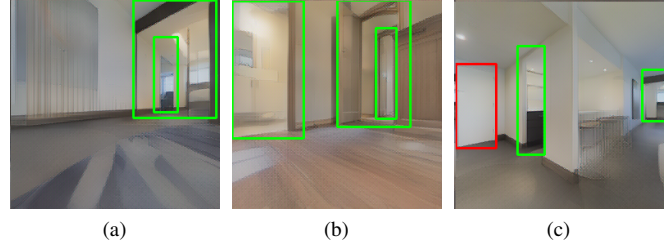


Fig. 1: A robot, navigating from a location to another, can observe the status (open or closed) of different doors. In this condition, door-status detection can be a difficult task as, from the robot point of view, doors can be nested (a–b), doors can be hidden in the wall (c), or instead of a door sometimes there are just passages (a–c). The bounding boxes of open (closed) doors, as identified by our method, are shown in green (red). For the remainder of this work, we follow the same colour schema.

to recognize its traversability (open or closed status) from visual perceptions, enabling the construction of predictive topological models.

In this work, we propose a method to endow a robot with high-performance door-detection capabilities that can be run in real-time during task-related autonomous navigation.

Door-status detection is particularly challenging for mobile robots operating indoor since clear and well-framed views of a door are seldom encountered during navigation. Figure 1 (a–c) depicts some typical instances of these challenges. While navigating, the robot can view nested doors (Fig. 1 (a–b)), doors that are only partially occluded (Fig. 1 (c)), or closed doors that are difficult to distinguish from their background (Fig. 1 (c)).

To tackle the above problem, our approach starts with the natural choice of modelling door-status detection as a variant of object detection (OD) performed with deep neural networks. However, customary object detection methods have important shortfalls when cast into the indoor navigation setting described above. Hence, our approach starts from object detection, but goes beyond it by providing solutions to what we identified as two main limitations.

First, OD methods are usually trained on large-scale datasets whose images are acquired from the point of view of a human user. As a result, training examples tend to follow a distribution that could be significantly different from the one generating the data perceived by a mobile robot. We show how popular datasets employed to train state-of-the-

art deep learning detectors [4], [5], do not properly represent the embodied perception constraints and uncertainty typically characterizing a mobile robot [6], thus causing generalization issues. Second, deep-learning OD modules are commonly trained with the main objective of obtaining a *general detector*. This model is trained once, stored, and is meant to work in every previously unseen environment. These practises are not optimal when considering the typical working conditions of a mobile robot. After an initial deployment phase, the robot is commonly used in the same environment for a long time, sometimes even for its entire life cycle. In such persistent conditions, the robot eventually observes the same doors multiple times, from different points of view, and under various environmental conditions. Also, different doors may present similar visual features (e.g., multiple doors of the same model). Against this operative background, the ability to generalise in new environments becomes less important, while correctly performing door-status detection in challenging images from the deployment environment becomes paramount.

To address the first limitation, we devise a method for acquiring a large visual dataset from multiple photorealistic simulations taking into account the robot’s perception model along navigation paths. This allows us to train a deep *general door-status detector* with examples following a distribution compliant with the robot’s perception capabilities. To deal with the second limitation, we exploit the robot’s operational conditions to tailor our general detector for a given target environment. We obtain what we call a *qualified detector*, whose performance substantially can improve from robot’s experience. Our solution relies on fine-tuning sessions [7]–[9] of the general detector with new examples from the target environment. These data can be collected, for example, during the robot installation phases or while the robot carries out its duties.

We evaluate our approach by assessing its satisfactory performance, also in the challenging cases exemplified in Fig. 1, with an extensive experimental campaign conducted in 10 simulated settings and in 3 real-world environments as perceived by a mobile robot during its deployment.

II. RELATED WORKS

As discussed in the previous section, the detection of doors and their status is an important ability needed by a robot to operate in indoor environments. Detecting a door’s location could be useful for several tasks, as *room segmentation* [10], i.e., to divide the map of the environment into semantically meaningful regions (rooms), to predict the shape of unobserved rooms [11], or to do *place categorization* [12], [13], which assigns to the rooms identified within the occupancy map a semantic label (e.g., *corridor* or *office*) according to their aspect.

Recent studies [2], [3] show how the door status affects the navigation capability of robots, and how recognizing it can optimize navigation, ultimately improving performance in long-term scenarios. The work of [3] models the periodic

environmental changes of a dynamic environment in a long-term run. The work presented in [2] proposes a navigation system for robots that operate for a long time in indoor environments with traversability changes.

Detecting doors in RGB images has been addressed as an OD task. Classical methods are based on the extraction of handcrafted features [14]–[16]. Deep learning end-to-end methods [17] provide significant improvements thanks to their capability of automatically learning how to characterize an object class, robustly to scale, shift, rotation, and exposure changes. As a significant example, the work of [18] describes a method for door detection with the goal of supporting and improving the autonomous navigation task performed by a mobile robot. A convolutional neural network is trained to detect doors in an indoor environment and its usage is shown to help a mobile robot to traverse passages in a more efficient way. Another approach, proposed in [19], focuses on robustly identifying doors, cabinets, and their respective handles in order to allow grasping by a robot. The authors use a deep architecture based on YOLO [9] to detect the Region Of Interest (ROI) of doors. This allows to obtain the handle’s location by focusing only on the area inside the door ROI.

These works are representative examples of methods addressing the door detection problem within a mobile robotics domain. However, as we discussed, they do not explicitly consider the point of view of a mobile robot or do not take advantage from the robot’s typical operational conditions. In the following we devise an approach to overcome such limits.

III. BUILDING A DOORS DATASET FOR MOBILE ROBOTS

One of the key prerequisites to exploit deep learning to synthesise an effective door-status detector for a mobile robot is the availability of a dataset consistent with its challenging perception model (see Fig. 1). The examples contained in the dataset should follow three main desiderata. Images (i) should represent different environments with different features, thus allowing the model to learn how to generalise; (ii) should contain doors as observed from a point of view similar to the one of a robot navigating in an indoor environment; (iii) should be taken from real environments or with an adequate level of photorealism.

A naïve, but impractical and time-consuming, way to comply with the above requirements would be to deploy a robot on the field and having it exploring different environments while acquiring image samples of doors. The large overheads of such a procedure are well-known and a popular alternative is to rely on simulations [20] or publicly available datasets.

Meeting the desiderata (i)-(iii) in simulation is not straightforward since these are often not explicitly developed inside available frameworks. For example, simulation tools popular in robotics such as Gazebo [21] or Unreal [22], while providing accurate physics modelling, fail to represent the realism and complexity of the real world. On the other side, public datasets as [4], [23], [24], do not well represent the point of view of a robot in its working conditions [6]. To address these issues, we resort to the widely used framework of Gibson [25], which provides highly-realistic visual

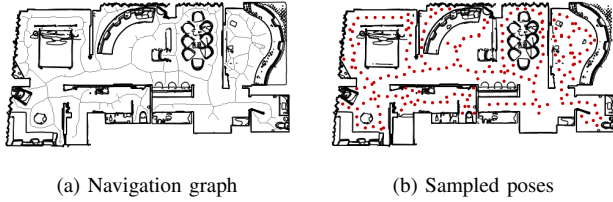


Fig. 2: Different phases of the pose extraction algorithm.

perceptions in conjunction with Matterport3D [26], a RGB-D dataset of 90 scans from real-world environments.

Given a simulated environment, we extract a set of poses that could describe views compatible with a mobile robot by applying a set of principles; the key ones include lying in the free space (feasibility), ensuring a minimum clearance from obstacles, and being along the shortest paths between key connecting locations in the environment’s topology. We achieve them with an extraction algorithm working in three phases: grid extraction, navigation graph extraction, and pose sampling.

The grid extraction phase aims at obtaining a 2D occupancy grid map, similarly to those commonly used by mobile robots for navigation. We start from the environment’s 3D mesh, and we aggregate obstacles from multiple cross-sections of the 3D mesh performed with parallel planes. The result is then manually checked for inaccuracies and artifacts produced during the procedure.

The *navigation graph* (shown in Fig. 2a) is a data structure that we use to represent the topology of the locations on the grid map that correspond to typical waypoints a robot occupies while navigating in the environment. We compute it from a Voronoi tessellation of the grid map by using obstacle cells as basis points [27], extracting graph edges from those locations that maintain maximum clearance from obstacles.

We then perform pose sampling on the navigation graph. The algorithm extracts from the graph a list of positions keeping a minimum distance D between them (this parameter controls the number and the granularity of the samples). A visual example of the algorithm’s results is shown in Fig. 2b.

To build the dataset we acquire an image from the points of view of a robot’s front-facing camera simulating its perceptions in the virtual environment from the sampled poses. Specifically, in each pose on the grid map, we acquire perceptions at two different height values (0.1 m and 0.7 m – to simulate different embodiments of the robots) and at 8 different orientations (from 0° to 315° with a step of 45°). Each acquisition includes the RGB image, the depth information, and the semantic data from Matterport3D. Since the semantic annotation of Matterport3D presents some inaccuracies, data labelling is manually performed by a human operator who specifies the door bounding boxes and the door status as open or closed.

We considered 10 different Matterport3D environments (small apartments or large villas with multiple floors and a heterogeneous furniture style) by setting $D = 1\text{m}$. The final

dataset we obtained is composed of 9363 examples, 5457 of which are positives and 3906 negatives. Note how our process to obtain the door detection dataset could easily be generalised to create any visual indoor data set for mobile robots by changing the image classification step.

IV. DOOR-STATUS DETECTION FOR MOBILE ROBOTS

In this section, we first detail how we synthesized a *General Detector* (GD , Section IV-A) using a dataset generated with the approach of Section III. Subsequently, leveraging the assumption that the environment e will not change in its core features (location and visual aspect of doors) during the robot’s long-term employment, we introduce our *Qualified Detector* for e (QD_e) by applying a procedure based on fine-tuning [7]–[9], [28] of the GD on additional data that, in our envisioned scenario, can be acquired and labelled during the first setup of the robot in e .

A. General Door-Status Detector

The general door-status detector we provide is based on DETR (DEtection TRansformer), a state-of-the-art deep-learning approach for object detection [28]. The method combines a CNN backbone based on ResNet [7] to produce a compact representation of an image and a transformer [29] to find complex relationships between the extracted features. We used a version of it that was pre-trained on the dataset COCO 2017 [4] and, to adjust for door-status detection, we chose the smallest configuration provided by the authors. It is composed of a ResNet-50 backbone, a transformer, and a 4-layers perceptron, for a total of 41 million parameters.

The model has one key hyper-parameter, N , which determines the fixed number of bounding boxes produced by the model for each image. As a consequence, to filter out the detected doors, we select the $n \leq N$ bounding boxes whose confidence is not below a threshold ρ_c . We tuned N considering the fact that it should not be too large but, at the same time, it should be higher than maximum number of detectable doors in any single image. After preliminary experimental tests, it was set to 10.

To train the general detector, we fixed the first two layers of the CNN backbone (as done in [28]) with the weights provided in the pre-trained model. We then re-trained the remaining layers with images taken from the dataset described in Section III. To achieve data augmentation, we generated additional samples by applying a random horizontal flip and resize transformation to a subset of the images (each training sample is selected for this procedure with probability of 0.5.)

B. Qualification of Door Detector on a Target Environment

Given an environment e we use a randomly sampled subset of the images collected in it to fine-tune the GD , obtaining the qualified detector QD_e . To be used in the fine-tuning procedure, these images need to be labelled specifying the bounding boxes and the status for each visible door. This task is rather time-expensive; yet it is required. In principle, we could use *pseudo-labels* automatically obtained by running the GD over the additional samples. Despite intriguing,

this approach turned out to be unsatisfactory for our door-status detection problem. The challenges introduced by the need to consider the robot’s perspective that we described in Section III make pseudo-labels not accurate enough for such an incremental learning method. From preliminary experiments, we empirically observed that fine-tuning GD with pseudo-labels obtained with it resulted into a QD whose performance was significantly degraded of about 20%. The study of methods to ease the burden of this task will be addressed as a part of our future works.

In our envisioned scenario, this data acquisition and labeling tasks can be carried out by a technician during the robot’s first installation in e or in a second phase by uploading the data to a remote server. Such a setup phase requires to build the map of the environment (either autonomously or with teleoperation) by observing the entirety of the working environment and is very relevant to many real-world installations of collaborative robots, as we recently experienced with extensive on-the-field testing in the use case of assistive robotics [30].

Finally, note that, while we focus here on a specific model GD based on DETR [28], this method to obtain a qualified detector QD is general and can be applied to other detectors and methods [8], [9].

V. EVALUATION IN SIMULATION

A. Experimental Settings

We evaluate our method using simulated data \mathcal{D} obtained, as described in Section III, from 10 different Matterport3D [26] environments. We test the performance of our detectors on each environment e independently. First, we train the general detector GD_{-e} using the dataset \mathcal{D}_{-e} , where $\mathcal{D} = \{\mathcal{D}_{-e}, \mathcal{D}_e\}$, \mathcal{D}_e contains all the instances acquired from poses sampled in environment e , and $\mathcal{D}_{-e} = \mathcal{D} \setminus \mathcal{D}_e$. Then, we randomly partition the first subset as $\mathcal{D}_e = \{\mathcal{D}_{e,1}, \mathcal{D}_{e,2}, \mathcal{D}_{e,3}, \mathcal{D}_{e,4}\}$, where each $\mathcal{D}_{e,i}$ contains the 25% of the examples from e , randomly selected.

While $\mathcal{D}_{e,4}$ is reserved for testing, the remaining subsets are used to perform a series of fine-tuning rounds to obtain the corresponding qualified door-status detectors. Specifically, we fine-tune GD_{-e} using these three additional data subsets: $\{\mathcal{D}_{e,1}\}$, $\{\mathcal{D}_{e,1}, \mathcal{D}_{e,2}\}$, and $\{\mathcal{D}_{e,1}, \mathcal{D}_{e,2}, \mathcal{D}_{e,3}\}$. We denote the obtained qualified detectors as QD_e^{25} , QD_e^{50} , and QD_e^{75} , respectively. The superscript denotes the percentage of data instances from e that are required to fine-tune the general door-status detector. Such a percentage can be interpreted as an indicator of the cost to acquire and label the examples. To give a rough idea, labelling the 25% of the dataset (approximately 150 images) took us an effort of about 1 hour.

We set the parameters of the door-status detector as $N = 10$ (number of bounding boxes) and $\rho_c = 0.75$ (confidence threshold). We conducted an extensive preliminary experimental campaign spanning different batch sizes ($\{1, 2, 4, 16, 32\}$) and the number of epochs ($\{20, 40, 60\}$) selecting 1 and 60 for the general detector and 1 and 40 for the qualified ones, respectively.

We measure performance with the average precision score (AP) used in the Pascal VOC challenge [5] by adjusting for a finer interpolation of the precision/recall curve to get a more conservative (in the pessimistic sense) evaluation. The AP is a popular evaluation metric widely adopted for object detection tasks, it represents the shape of the precision/recall curve as the mean precision over evenly distributed levels of recall. To accept a true positive, the bounding box computed by the network must exhibit an Intersection Over Union area (IOU) with one true bounding box above a threshold ρ_a , empirically set to 75%.

B. Results

Table I reports the mean AP scores (averaged over the 10 environments) reached by the 4 detectors divided by label (closed door, and open door), the average increments (with respect to the detector immediately above in table) obtained with fine-tuning, and the standard deviation (σ). We also report the AP scores for every environment in Fig. 3. These results expose the trade-off between performance increase (via fine-tuning) and data collection costs.

| Exp. | Label | AP | σ | Increment | σ |
|-------------|--------|----|----------|-----------|----------|
| GD_{-e} | Closed | 37 | 15 | – | – |
| | Open | 55 | 10 | – | – |
| QD_e^{25} | Closed | 59 | 16 | 68% | 48 |
| | Open | 66 | 9 | 23% | 24 |
| QD_e^{50} | Closed | 69 | 13 | 22% | 21 |
| | Open | 73 | 8 | 11% | 8 |
| QD_e^{75} | Closed | 77 | 9 | 12% | 10 |
| | Open | 77 | 7 | 5% | 5 |

TABLE I: Average AP in Matterport3D environments.

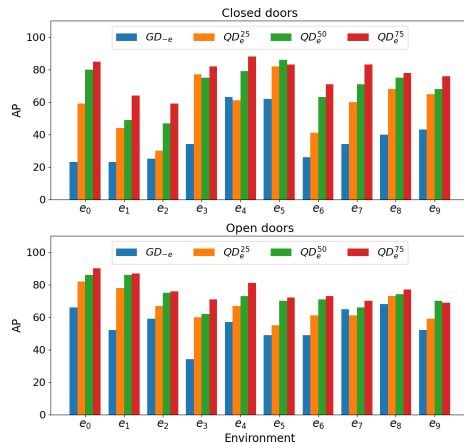


Fig. 3: AP scores in Matterport3D environments.

Results from Table I suggest that a general detector GD_{-e} (blue) have acceptable performances when trained with a dataset \mathcal{D}_{-e} representing the robot point of view (Section III). More interestingly, qualified detectors achieve a steep increase in performance. Unsurprisingly, the performance improves with more data (and acquisition costs) from QD_e^{25} to QD_e^{75} . However, it can be seen how QD_e^{25} , despite requiring a little effort in manual labelling, obtains the highest performance increase. From a practical perspective, this

shows how the availability of *a few* labelled examples from the robot target environment could be a good compromise between performance and costs to develop an environment-specific door-status detector. This suggests that the number of examples that have to be collected and labelled on the field can be limited, thus promoting the applicability of our proposed framework. An example of this is shown in Fig. 4, where it can be seen how a QD_e^{25} fixes the mistakes of its corresponding general detector GD_{-e} in challenging images with nested or partially observed doors.

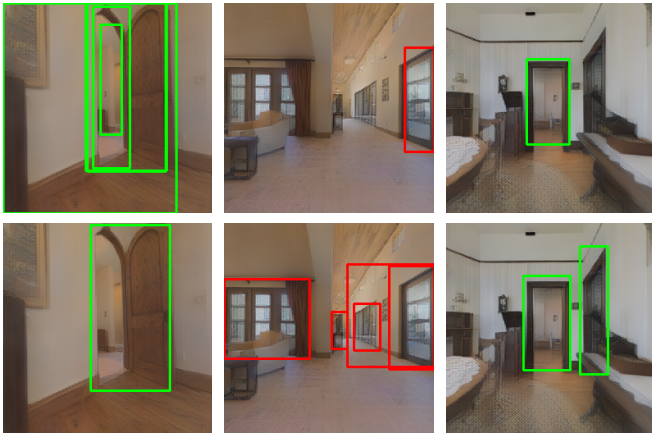


Fig. 4: Predictions of GD_{-e} (top row) compared to QD_e^{25} (bottom row) in Matterport3D environments.

VI. EVALUATION IN THE REAL WORLD

A. Experimental Settings

In this section, we evaluate the performance of our method with a real robot by using images collected by a Giraff-X platform [30] during a teleoperated exploration of 3 single-floor indoor environments from two buildings in our campus, containing multiple rooms. Images were extracted from the robot’s perceptions during navigation at 1 fps.

First, we consider two general detectors. One is trained with simulated data \mathcal{D} , as in the previous section but with all the 10 environments. Another one is trained with real-world images from the publicly available *DeepDoors2* dataset (DD2) [24], which features 3000 images of doors that we re-labelled to include the ground truth for challenging examples not originally provided. Comparing these two general detectors, we aim at assessing the advantages of training with a dataset following the principles we proposed in Section III instead of relying of mainstream datasets for classical object detection.

Subsequently, following the same steps of Section V-A, we qualify both GD s by using the 25, 50, and 75% of data collected in the three real environments.

B. Evaluation metrics

Analogously to what done in simulation, we report the AP scores, but we argue that the real-world evaluation of our method can be conducted also with additional metrics, which

are more representative of the actual application domain where door-status detection is meant to be cast.

The AP (as well as other metrics used in computer vision) presents some limitations when used in our context. Such a metric considers as false positives multiple bounding boxes assigned to the same door. However, a robot can easily disambiguate this by leveraging additional data such as its estimated pose and the map of the environment. Although an erroneous localisation of the bounding box of a door penalises the AP, it has little effect in practice. Moreover, the AP is very marginally affected by a wrong detection of the door status if the bounding box is sufficiently accurate due to the fact that different labels are treated as two independent object classes. However, misleading a closed passage for an open one (and vice versa) can have potentially catastrophic consequences when the robot translates such an information into actions.

To address this shortcoming and better capture performance in our robotic setting, we introduce three additional metrics. Consider a door i in a given image. If multiple bounding boxes are matched to i , where matching means $IOU \geq \rho_a$, the one with the maximum above-threshold (ρ_c) confidence is selected. If the status of the door is correctly identified, we consider it as a true positive (TP). Otherwise, we classify it as a False Positive (FP). All the remaining bounding boxes matched to i are, as per our previous considerations, ruled out from the evaluation. Finally, when a bounding box does not meet the IOU condition with any door in the image, we count it as a Background False Detection (BFD). A False Positive and a Background False Detection are errors that can play very different roles inside a robotic use case. While the first is likely to affect the robot’s decisions, the second one might increase the uncertainty in the robot world-model. We scale the above metrics using the true number of doors in the testing set, denoted as GT , thus obtaining $TP\% = TP/GT$, $FP\% = FP/GT$, and $BFD\% = BFD/GT$.

C. Results

Table II compares the average AP of the GD trained with DD2 with that trained with our dataset \mathcal{D} . Intuitively, a model trained with real-world data (such as those featured in DD2) should have higher performance when used with real-world data, if compared with a model trained with simulated data (as \mathcal{D}). However, Table II shows how the GD and QD s trained with \mathcal{D} have higher performance than those trained with DD2. This is because training images of \mathcal{D} , collected from the simulated point of view of a robot, better represent the actual distribution of robot perceptions, allowing us to fill, to some extent, the sim-to-real gap.

Moreover, Table II shows that the fine-tuning operation to qualify GD_{-e} to the target environment works remarkably well also when used in real-world conditions. The performance of QD s is similar to that obtained in the far less challenging dataset of Table I. Most importantly, the performances of QD_e^{25} corroborate our findings from Section V-A, confirming how few additional examples can

| Exp. | Label | DeepDoors2 | | | | Our dataset | | | |
|-------------|--------|------------|----------|------|----------|-------------|----------|------|----------|
| | | AP | σ | Inc. | σ | AP | σ | Inc. | σ |
| GD_{-e} | Closed | 7 | 3 | - | - | 15 | 10 | - | - |
| | Open | 24 | 2 | - | - | 39 | 11 | - | - |
| QD_e^{25} | Closed | 49 | 18 | 672% | 371 | 63 | 5 | 484% | 372 |
| | Open | 53 | 13 | 129% | 39 | 67 | 10 | 74% | 22 |
| QD_e^{50} | Closed | 64 | 7 | 42% | 51 | 74 | 6 | 17% | 6 |
| | Open | 64 | 4 | 24% | 26 | 78 | 5 | 19% | 12 |
| QD_e^{75} | Closed | 65 | 8 | 2% | 7 | 78 | 7 | 5% | 2 |
| | Open | 75 | 1 | 18% | 5 | 85 | 2 | 1% | 5 |

TABLE II: Average AP in real-world environments when *DeepDoors2* and our dataset are used to train the *GD*.

induce a significant increase in performances. Beyond the improvements observed in the average scores, QD_e^{25} managed to provide correct door-status detection in very challenging cases, in Fig. 5 we report some representative examples. As it can be seen, our detectors correctly recognised cases with nested doors, partially visible frames, and narrow side views. Another relevant example is in the second image (top row) of Fig. 5, where the qualified model succeeds in detecting a white closed door in the background while, at the same time, not making a false detection of the white wardrobe doors on the right.



Fig. 5: Challenging doors detected by QD_e^{25} in the real environments e_1 , e_2 , and e_3 (ordered by columns).

Table III reports the detailed results, for all three environments, of the metrics we defined in Section VI-B.

| Env. | Exp. | <i>GT</i> | <i>TP</i> ($TP\%$) | <i>FP</i> ($FP\%$) | <i>BFD</i> ($BFD\%$) |
|-------|-------------|-----------|----------------------|----------------------|------------------------|
| e_1 | GD_{-e} | 235 | 83 (35.3) | 18 (7.7) | 33 (14) |
| | QD_e^{25} | 235 | 171 (72.8) | 13 (5.5) | 32 (13.6) |
| | QD_e^{50} | 235 | 190 (80.9) | 5 (2.1) | 22 (9.4) |
| | QD_e^{75} | 235 | 201 (85.9) | 4 (1.7) | 20 (8.5) |
| e_2 | GD_{-e} | 269 | 106 (39.4) | 23 (8.6) | 37 (13.8) |
| | QD_e^{25} | 269 | 210 (78.1) | 15 (5.6) | 34 (12.6) |
| | QD_e^{50} | 269 | 227 (84.4) | 8 (3) | 25 (9.3) |
| | QD_e^{75} | 269 | 242 (90) | 7 (2.6) | 25 (9.3) |
| e_3 | GD_{-e} | 327 | 79 (24.2) | 29 (8.9) | 79 (24.2) |
| | QD_e^{25} | 327 | 230 (70.3) | 28 (8.6) | 113 (34.6) |
| | QD_e^{50} | 327 | 252 (77.1) | 14 (4.3) | 55 (16.8) |
| | QD_e^{75} | 327 | 267 (81.7) | 9 (2.8) | 43 (13.2) |

TABLE III: Extended results in the real-world environments.

The results show that *GD*, although it has a low number of wrong predictions (*FP* and *BFD*), is capable of detecting only a few of the *GT* doors in the images (*TP*). On

the contrary, *QDs* dramatically improve performance, with QD_e^{25} showing a $TP\%$ of 74% on average.

Among the three environments considered, we argue that e_3 is the more challenging, as it can be seen by the higher number of *BFD*. To cope with this, there are two possible directions. First, increasing the number of manually labelled examples reduces *BFD* (as can be seen already with QD_e^{50}). Alternatively, adopting a more conservative selection rule by increasing the confidence threshold ρ_c , at the cost of slightly reducing the number of *TP*. In Fig. 6, we show how $TP\%$, $FP\%$, and $BFD\%$ for QD_e^{25} change when varying ρ_c in e_3 . Such an instance confirms how $\rho_c = 0.75$ is an acceptable trade-off among $TP\%$ (high) and $BFD\%$ (low) for such a detector.

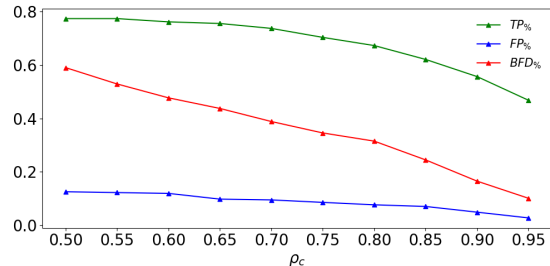


Fig. 6: $TP\%$, $FP\%$, and $BFD\%$ obtained by QD_e^{25} for increasing confidence thresholds.

Finally, we assessed the real-time feasibility of our solution by running our detectors on the Giraff-X platform, which is equipped with an edge-computing GPU (NVIDIA Jetson TX2). The experiment showed how both the general and qualified detectors could be run in the ROS framework with an acceptable real-time performance of approximately 0.4 fps.

VII. CONCLUSIONS

In this work, we have presented a door-status detection method for autonomous mobile robots. Our method, based on a deep learning architecture, allows robots to localize and distinguish between open or closed doors also in challenging situations. To train our model, we built a dataset of labelled images from photorealistic simulations taking into account the point of view of a mobile robot. We then proposed to fine-tune a general model into a qualified one to increase performance in the working environment of the robot. The source code of our simulation framework, the door detectors and all the datasets are available in a public repository¹.

Future work will investigate how to quantify and reduce the effort needed for labelling enough new examples to qualify a general detector. Furthermore, we will study approaches to perform online fine-tuning reducing the need of human intervention to obtain new labelled examples. The final goal is to have a robot can learn with experience to better distinguish features, such as doors, in its operational environment.

¹<https://github.com/aislabunimi/door-detection-long-term>

REFERENCES

- [1] L. Kunze, N. Hawes, T. Duckett, M. Hanheide, and T. Krajník, "Artificial Intelligence for Long-Term Robot Autonomy: A Survey," *IEEE RA-L*, vol. 3, no. 4, pp. 4023–4030, 2018.
- [2] L. Nardi and C. Stachniss, "Long-term robot navigation in indoor environments estimating patterns in traversability changes," in *Proc. ICRA*, 2020, pp. 300–306.
- [3] T. Krajník, J. P. Fentanes, J. M. Santos, and T. Duckett, "Fremen: Frequency map enhancement for long-term mobile robot autonomy in changing environments," *IEEE Trans. Rob.*, vol. 33, no. 4, pp. 964–977, 2017.
- [4] T.-Y. Lin, M. Maire, S. Belongie, J. Hays, P. Perona, D. Ramanan, P. Dollár, and C. L. Zitnick, "Microsoft coco: Common objects in context," in *Proc. ECCV*, D. Fleet, T. Pajdla, B. Schiele, and T. Tuytelaars, Eds. Cham: Springer International Publishing, 2014, pp. 740–755.
- [5] M. Everingham, L. V. Gool, C. K. I. Williams, J. M. Winn, and A. Zisserman, "The pascal visual object classes (voc) challenge," *Int. J. Comput. Vision*, vol. 88, pp. 303–338, 2009.
- [6] N. Sünderhauf, O. Brock, W. Scheirer, R. Hadsell, D. Fox, J. Leitner, B. Upcroft, P. Abbeel, W. Burgard, M. Milford *et al.*, "The limits and potentials of deep learning for robotics," *Int. J. Rob. Res.*, vol. 37, no. 4-5, pp. 405–420, 2018.
- [7] K. He, X. Zhang, S. Ren, and J. Sun, "Deep residual learning for image recognition," in *Proc. CVPR*, June 2016.
- [8] S. Ren, K. He, R. Girshick, and J. Sun, "Faster r-cnn: Towards real-time object detection with region proposal networks," *IEEE Trans. Pattern Anal. Mach. Intell.*, vol. 39, no. 6, pp. 1137–1149, 2017.
- [9] J. Redmon, S. Divvala, R. Girshick, and A. Farhadi, "You only look once: Unified, real-time object detection," in *Proc. CVPR*, June 2016.
- [10] R. Bormann, F. Jordan, W. Li, J. Hampp, and M. Hägele, "Room segmentation: Survey, implementation, and analysis," in *Proc. ICRA*, 2016, pp. 1019–1026.
- [11] M. Luperto, F. Amadelli, and F. Amigoni, "Completing robot maps by predicting the layout of rooms behind closed doors," in *Proc. ECMR*, 2021.
- [12] P. Espinace, T. Kollar, A. Soto, and N. Roy, "Indoor scene recognition through object detection," in *Proc. ICRA*, 2010, pp. 1406–1413.
- [13] N. Sünderhauf, F. Dayoub, S. McMahon, B. Talbot, R. Schulz, P. Corke, G. Wyeth, B. Upcroft, and M. Milford, "Place categorization and semantic mapping on a mobile robot," in *Proc. ICRA*, 2016, pp. 5729–5736.
- [14] N. Kwak, H. Arisumi, and K. Yokoi, "Visual recognition of a door and its knob for a humanoid robot," in *Proc. ICRA*, 2011, pp. 2079–2084.
- [15] I. Monasterio, E. Lazkano, I. Rañó, and B. Sierra, "Learning to traverse doors using visual information," *Math. Comput. Simul.*, vol. 60, no. 3, pp. 347–356, 2002.
- [16] X. Yang and Y. Tian, "Robust door detection in unfamiliar environments by combining edge and corner features," in *Proc. CVPR*, 2010, pp. 57–64.
- [17] A. Voulodimos, N. Doulamis, A. Doulamis, and E. Protopapadakis, "Deep learning for computer vision: A brief review," *Comput. Intell. Neurosci.*, vol. 2018, 2018.
- [18] W. Chen, T. Qu, Y. Zhou, K. Weng, G. Wang, and G. Fu, "Door recognition and deep learning algorithm for visual based robot navigation," in *Proc. ROBIO*, 2014, pp. 1793–1798.
- [19] A. Llopart, O. Ravn, and N. A. Andersen, "Door and cabinet recognition using convolutional neural nets and real-time method fusion for handle detection and grasping," in *Proc. ICCAR*, 2017, pp. 144–149.
- [20] J. Collins, S. Chand, A. Vanderkop, and D. Howard, "A review of physics simulators for robotic applications," *IEEE Access*, 2021.
- [21] N. Koenig and A. Howard, "Design and use paradigms for gazebo, an open-source multi-robot simulator," in *Proc. IROS*. IEEE, 2004, pp. 2149–2154.
- [22] S. Carpin, M. Lewis, J. Wang, S. Balakirsky, and C. Scrapper, "Usarsim: a robot simulator for research and education," in *Proc. ICRA*. IEEE, 2007, pp. 1400–1405.
- [23] J. Deng, W. Dong, R. Socher, L.-J. Li, K. Li, and L. Fei-Fei, "Imagenet: A large-scale hierarchical image database," in *Proc. CVPR*, 2009, pp. 248–255.
- [24] J. Ramôa, V. Lopes, L. Alexandre, and S. Mogo, "Real-time 2d–3d door detection and state classification on a low-power device," *SN Appl. Sci.*, vol. 3, 05 2021.
- [25] F. Xia, A. R. Zamir, Z. He, A. Sax, J. Malik, and S. Savarese, "Gibson env: Real-world perception for embodied agents," in *Proc. CVPR*, 2018, pp. 9068–9079.
- [26] A. X. Chang, A. Dai, T. A. Funkhouser, M. Halber, M. Nießner, M. Savva, S. Song, A. Zeng, and Y. Zhang, "Matterport3d: Learning from RGB-D data in indoor environments," 2017.
- [27] S. Thrun and A. Bücken, "Integrating grid-based and topological maps for mobile robot navigation," in *Proc. AAAI*, 1996, pp. 944–951.
- [28] N. Carion, F. Massa, G. Synnaeve, N. Usunier, A. Kirillov, and S. Zagoruyko, "End-to-end object detection with transformers," in *Proc. ECCV*, 2020.
- [29] A. Vaswani, N. Shazeer, N. Parmar, J. Uszkoreit, L. Jones, A. N. Gomez, Ł. Kaiser, and I. Polosukhin, "Attention is all you need," in *Proc. NIPS*, 2017, pp. 5998–6008.
- [30] M. Luperto, M. Romeo, J. Monroy, J. Renoux, A. Vuono, F.-A. Moreno, J. Gonzalez-Jimenez, N. Basilico, and N. A. Borghese, "User feedback and remote supervision for assisted living with mobile robots: A field study in long-term autonomy," *Robotics and Autonomous Systems*, vol. 155, p. 104170, 2022.